Investigation of ICRF Heating Effect in Anchor Region on GAMMA 10/PDX*)

Mafumi HIRATA, Junpei ITAGAKI, Ryuya IKEZOE[1)], Makoto ICHIMURA, Shuhei SUMIDA, Seowon JANG, Koki IZUMI, Atsuto TANAKA, Yushi KUBOTA, Ryo SEKINE, Hiroki KAYANO, Mizuki SAKAMOTO and Yousuke NAKASHIMA

Plasma Research Center, University of Tsukuba, Tsukuba 305-8577, Japan
[1)]*Research Institute for Applied Mechanics, Kyushu University, Kasuga 816-8580, Japan*

(Received 30 September 2018 / Accepted 3 February 2019)

To investigate end-loss plasma control, several heating operations were carried out using ion-cyclotron range of frequency (ICRF) heating systems in GAMMA 10/PDX. In anchor region, one of the important heating positions to control the end loss particle and heat fluxes, excited ICRF waves are measured as the density fluctuations using an upgraded reflectometer system and the detailed radial profiles are observed. The efficiency of anchor heating was changed using the phase control between two antennas installed in the anchor and/or the central region. The interference of two waves during a phase-control ICRF heating has been directly measured inside the plasma. In addition, several phase dependencies were observed using absorption methods with photodiode in anchor region.

Keywords: GAMMA 10/PDX, ICRF, anchor region, phase control, microwave reflectometer, absorption method

DOI: 10.1585/pfr.14.2402055

1. Introduction

In the GAMMA 10/PDX tandem mirror, divertor simulation experiments have been performed in the open magnetic field at the west end region [1]. High particle and heat fluxes in the end region along the magnetic field line are required. To control the end loss ions, the ion-cyclotron range of frequency (ICRF) antennas in the central cell, the anchor cells, and the west plug/barrier cells have been used in several combinations [2].

In a standard operation, the ICRF waves excited in the central cell are used for an initial plasma production, ion hating in the central and anchor region, and sustaining MHD stability [3]. The obtained ion temperature is several keV in the perpendicular direction to magnetic field lines at central region and a few hundred eV in the parallel direction at end region, and the end-loss ion flux is on the order of $10^{22}\,\mathrm{m^{-2}s^{-1}}$. Additional heating in the anchor or barrier region can control the end loss ions and/or the heat fluxes [4, 5]. For example, a simultaneous production of high density plasma in both anchor cells leads to an increase of density in the central cell, and as a result, an end loss flux more than $10^{23}\,\mathrm{m^{-2}s^{-1}}$ has been obtained.

Though plasma production in the anchor cell is one of the important issues for improving the performance of the end loss plasma, the minimum-B anchor region has a complicated structure of magnetic field and a limited space for measurements. In this paper, investigation of relationship between excited ICRF waves and plasma production are discussed. ICRF waves are measured as density fluctuations using an upgraded reflectometer system [6]. To modify the strength of ICRF waves in the anchor region, control of phase difference between RF currents on two ICRF antennas was utilized. Several phase dependencies related to ion and/or electron temperature were observed using absorption methods with photodiode in anchor region.

2. Experimental Apparatus

2.1 GAMMA 10/PDX and ICRF Heating Systems

This study has been carried out in GAMMA 10/PDX [1–3], which is a minimum-B anchored tandem mirror with outboard axisymmetric plug/barrier cells. The central cell has a length of 5.6 m and the magnetic field intensity at the midplane is 0.4 T with a mirror ratio of 5. The fixed 8-segmented limiter with a diameter of 36 cm is installed near the midplane [7]. Similarly, a length, the magnetic field intensity at the midplane, and a mirror ratio of the minimum-B anchored cell are 4.7 m, 0.6 T, and 3, respectively.

There are seven sets of ICRF antennas in the GAMMA 10/PDX central and anchor cells as shown in Fig. 1 (a). ICRF waves are exited using three ICRF systems as called RF1, RF2 and RF3. RF1 and RF2 have two outputs and RF3 has one output. The target plasma initiated with magnetoplasma dynamic guns is produced and

author's e-mail: mafumi@prc.tsukuba.ac.jp

*) This article is based on the presentation at the 12th International Conference on Open Magnetic Systems for Plasma Confinement (OS2018).

sustained by RF1 (9.9 and 10.3 MHz, ~80 kW) using east and west Nagoya Type III antennas in central cell near the mirror throat (E-Type III, W-Type III). In a standard operation, RF2 (6.36 MHz, ~80 kW) using east and west double half-turn antennas in central cell (E-DHT, W-DHT) is employed for producing bulk hot ions in the central region. For direct heating of the anchor region, one double-arc-type (DAT) shape antenna is installed in the east anchor cell on the inner side (the side of central cell, EAI-DAT) and two antennas (WAI-DAT, WAO-DAT) are installed in the west anchor cell on the inner and outer side with midplane (Z = 5.2 m) as shown Figs. 1 (a) (b). The frequencies of the ICRF systems are varied according to the purpose of the experiment.

2.2 Diagnostics

Microwave reflectometry is widely used for density fluctuation measurement in fusion experimental devices because of its superior advantages such as compactness and non-perturbative measurement [8]. A heterodyne microwave reflectometer is installed in the GAMMA 10/PDX west anchor cell (Fig. 1 (c)). Two horn antennas, for transmitting and receiving microwave, are located inside the vacuum chamber, which are 0.27 m away from the center at midplane in the X-Y plane. The microwave from a voltage controlled oscillator (VCO, VO4280X/00, SIVERSIMA) is launched with O-mode polarization. The VCO covers from 8.4 to 13.5 GHz corresponding to the cut-off radius r_c from r_c/a~0.7 to the center of plasma, where the plasma radius a is ~0.15 m at the midplane of the anchor mirror field. High frequency-sweeping of up to 100 kHz is possible. The received microwave fed into the heterodyne circuit is mixed with the reference microwave, and the in-phase and quadrature signals are obtained by the IQ detector.

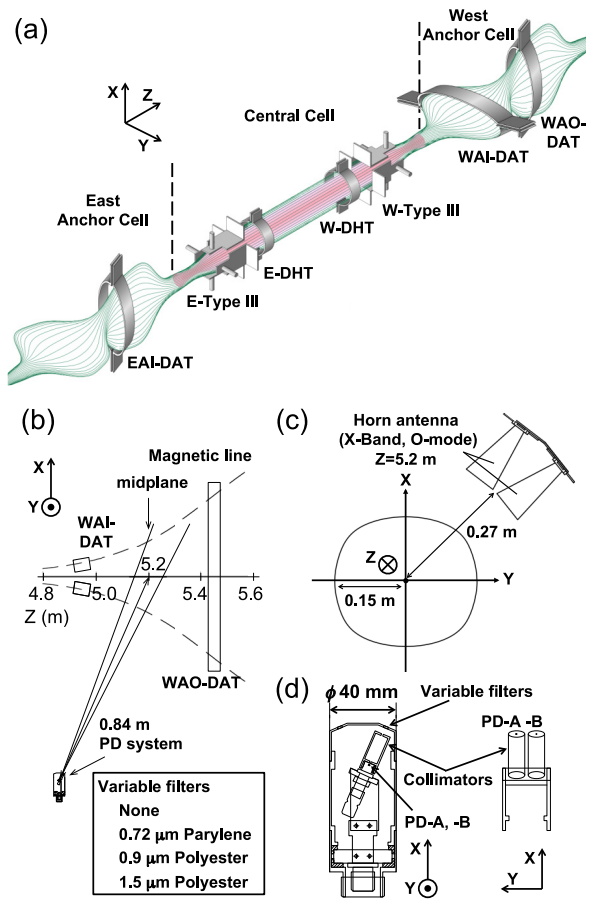

Fig. 1 Schematic drawing of (a) the magnetic field configuration and ICRF antennas in the GAMMA 10/PDX central and anchor cells, (b) WAI- and WAO-DAT antennas, the magnetic field lines, and location of PD system in west anchor cell, (c) location of horn antennas for microwave reflectometer, (d) details of PD system, respectively.

Semiconductor detectors are able to use even in complex magnetic fields like the GAMMA 10/PDX anchor cell and have sensitivity both to X-ray with electron energy information and to charge-exchange neutral particles with ion energy information. Two photodiodes (PD-A: AXUVHS5/ PD-B: UVGHS5, IRD) were installed with the center of west anchor cell as the field of view (Figs. 1 (b) (d)). Sensitive area of these detectors is 1 mm^2 and SiO_2 passivating layer of PD-A and PD-B is 6-8 and 40-150 nm, respectively. Absorption method is one of energy analysis methods of particle and radiation [9, 10]. Due to the difference in the passivating layer, the intensity ratio of PD-B to PD-A ($I_{PD\text{-}B}/I_{PD\text{-}A}$) corresponds to the electron temperature and/or the ion temperature, without depending on the number of electrons, ions and neutral particles. Variable filters noted on the Fig. 1 (b) change the proportion and energy of X-rays and charge-exchange neutral particles incident on PD-A and PD-B.

3. Experimental Results and Discussions

ICRF heating effect in anchor region is investigated using three different ICRF heating conditions. First, density fluctuations in the west anchor midplane associated with the ICRF wave are observed on the standard operation (Fig. 2), where RF1 with 9.9, 10.3 MHz on E- and W-Type III is used for plasma production and the anchor ion

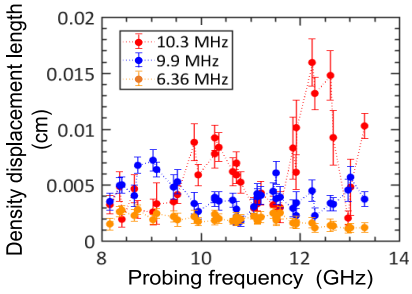

Fig. 2 Radial profile of the density displacement length due to the density fluctuation associated with the ICRF waves of 6.36, 9.9, and 10.3 MHz, respectively.

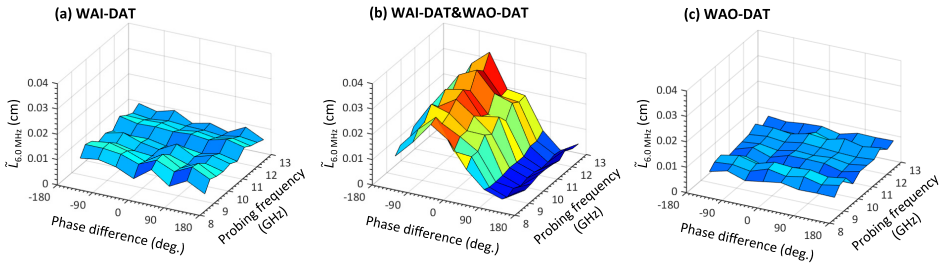

Fig. 3 Probing frequency dependence, corresponds to radial distribution, of density fluctuation length related to the relative phase difference of 6 MHz ICRF wave. The antenna for exciting the ICRF wave is temporally switched to (a) WAI-DAT, (b) WAI- and WAO-DAT, and (c) WAO-DAT within one discharge.

heating, and RF2 with 6.36 MHz on E- and W-DHT is used for the ion heating in central region. During the discharge duration of 200 ms, the probing frequency was cyclically swept with the waveform consisting of 10-step frequencies to obtain a fine radial distribution of density fluctuations. Figure 2 shows density displacement lengths derived from the phase fluctuation of microwave, $\lambda_{\rm eff}\ \delta\phi/4\pi$, where $\lambda_{\rm eff}$ is the effective wavelength at the cutoff and $\delta\phi$ is phase fluctuation amplitude. The data were obtained using four identical discharges. The wave structures of 9.9, 10.3 MHz used for ion cyclotron heating in the anchor region are revealed to have at least two peaks in the radial direction, which are different from the rather flat wave structures in the central cell. Since the wavelength of ICRF is the device scale at the density of GAMMA 10/PDX, its structure is strongly influenced by boundary conditions. As the major axis of the elliptically-shaped nonaxisymmetric magnetic field is 3 times longer than the plasma diameter at the central cell, there is a possibility to have a higher order radial structure even under a similar density, which is also indicated by a three-dimensional full wave calculation. Then, to connect to the elliptically elongated region located at both sides, the wave structure in the anchor midplane can be different from the structure in the central cell.

For efficient utilization of ICRF heating power, the wave power should be localized the wave at the resonance region. By interfering two waves, we have succeeded in such a power deposition control in GAMMA 10/PDX. The effects of the phase control have been studied with global plasma parameters so far. In this study, we have directly measured the wave interference inside the plasma using a microwave reflectometer. To exclude the wave attenuation effect by resonance, ICRF waves with 6.0 MHz, having no resonance layer in the anchor region, are excited on WAI- and WAO-DAT. The results are shown in Fig. 3. It is seen that the density fluctuation length of 6.0 MHz changes sinusoidally with the phase difference over the entire range of the measured probing frequency during the interference. The shortest density fluctuation length is smaller than those excited with a single antenna. The longest length is more than 2 times as that of the single antenna excitation.

To investigate the influence of change in ICRF power

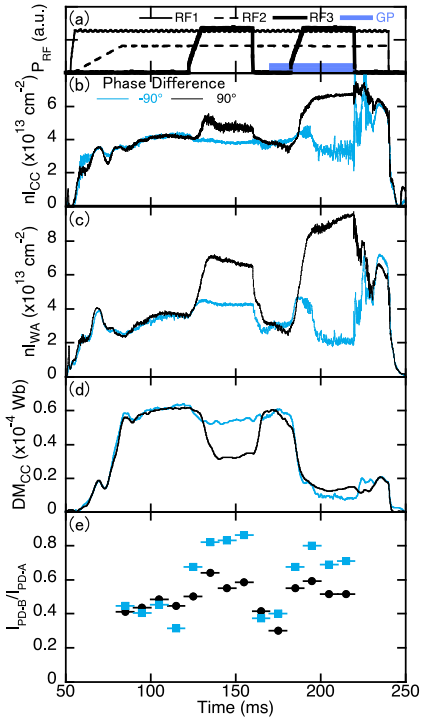

Fig. 4 Temporal evolution of (a) ICRF incident power for each antenna, and gas injection timing, the line density at (b) central cell and (c) west anchor cell, (d) diamagnetism in central cell, and (e) PDs intensity ratio under the conditions of phase difference between W-Type III and WAI-DAT are −90 and 90 degrees, respectively.

due to wave interference on plasma, phase control using ICRF wave of 10.3 MHz was performed between W-Type III and WAI- or WAO-DAT antennas. RF3 on WAI- or WAO-DAT antennas was powered twice and additional gas puffs (GP) was used the second time (Fig. 4 (a)). When RF3 was applied on WAI-DAT with a relative phase difference of 90 degrees to W-Type III, the line density of the west anchor cell ($nl_{\rm WA}$) increased, accompanied by the increase in that of the central cell ($nl_{\rm CC}$) (Figs. 4 (b) (c)). Further increase of the density in both cells was observed during the gas injection. Due to the increase of the line density, the diamagnetism in central cell ($DM_{\rm CC}$) tends to

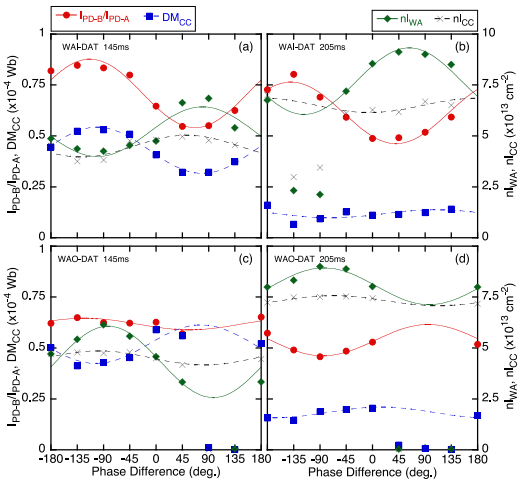

Fig. 5 Dependence of phase difference on nl_{WA}, nl_{CC}, DM_{CC} and $I_{PD\text{-}B}/I_{PD\text{-}A}$ during additional ICRF wave on (a) (b) WAI-DAT and (c) (d) WAO-DAT. In (b) (d), additional gas injection was performed.

decrease (Fig. 4 (d)). On the contrary, $I_{PD\text{-}B}/I_{PD\text{-}A}$ tends to increase regardless increase or decrease in nl_{WA} during the applied RF3 (Fig. 4 (e)). In this experiment, measurement of the PD detector was carried out using 0.9 mm Polyester. Under this condition, increase of $I_{PD\text{-}B}/I_{PD\text{-}A}$ suggests an increase in electron and/or ion energy in the anchor cell.

The dependences of these parameters on the phase difference during the wave interference (145 and 205 ms) are shown in Fig. 5. Though discharge was discontinued under some condition, each parameter varied approximately sinusoidally according to the phase difference. As an overall characteristic, nl_{CC} shows the same phase dependence with nl_{WA}, while DM_{CC} and $I_{PD\text{-}B}/I_{PD\text{-}A}$ show antiphase dependence with nl_{WA}.

Comparing the dependences between WAI-DAT and WAO-DAT, all the dependences shifted about π with holding relative relationships among the parameters. This shift can be explained by the difference in the geometrical conditions between the antenna and the resonance region at anchor cell. During the gas injection, nl_{WA} and nl_{CC} rise and DM_{CC} remarkably decreased, while $I_{PD\text{-}B}/I_{PD\text{-}A}$ is not changed much as expected; $I_{PD\text{-}B}/I_{PD\text{-}A}$ is less affected by the density. In the case of WAO-DAT, $I_{PD\text{-}B}/I_{PD\text{-}A}$ is small and the phase dependence is not strong, so it is considered that the energy of electrons and/or ions is low compared with the case of WAI-DAT.

4. Summary

Under a standard heating operation, a fine radial distribution of density fluctuations accompanied by the ICRF waves was obtained. The interference of two waves during a phase-control ICRF heating has been directly measured as the density fluctuation inside the plasma using the microwave reflectometer. The intensity ratio of PD detectors suggested the increase of ion and/or electron energy locally in the anchor region. To clarify the PD's data, it is necessary to improve S/N ratio, to measure the spatial distribution, and to evaluate the sensitivity on X-ray and charge-exchange neutral particles. Furthermore, the wave distribution analysis under the ICRF heating conditions is a future task because of the change in density distribution and the occurrence of wave attenuation.

Acknowledgments

The authors would like to thank the GAMMA 10 group at the University of Tsukuba for their collaboration in the experiments and for helpful discussion. This work was partly supported by the bidirectional collaborative research program of the National Institute for Fusion Science, Japan (NIFS14KUGM086 and NIFS17KUGM132).

[1] Y. Nakashima *et al.*, Nucl. Fusion **57**, 116033 (2017).
[2] R. Ikezoe *et al.*, Fusion Sci. Technol. **68**, 63 (2015).
[3] M. Ichimura *et al.*, Nucl. Fusion **28**, 799 (1988).
[4] S. Sumida *et al.*, Fusion Sci. Technol. **68**, 136 (2015).
[5] S. Jang *et al.*, AIP Conf. Proc. **1771**, 030011 (2016).
[6] H. Hojo *et al.*, J. Plasma Fusion Res. **69**, 1043 (1993).
[7] M. Hirata *et al.*, Trans. Fusion Sci. Technol. **63**, 247 (2013).
[8] A. Ejiri *et al.*, JPS Conf. Proc. **1**, 015038 (2014).
[9] M. Hirata *et al.*, Rev. Sci. Instrum. **66**, 2311 (1995).
[10] M. Hirata *et al.*, Trans. Fusion Sci. Technol. **39**, 281 (2001).